3 ZHANG, L., CHANDLER, P. J., TOWNSEND, P. D., and LAMA, F. L.: 'Structure property relationships in surface modified ceramics' *in* MCHARGUE, C., KOSSOWSKY, R., and HOFER, W. O. (Ed.) (Kluwer Academic, Dordrecht, 1989), pp. 371–378
4 CHANDLER, P. J., ZHANG, L., and TOWNSEND, P. D.: 'High temperature annealing of He^+ ion-implanted quartz optical waveguides', *Nuclear Instruments and Methods in Physics Research*, 1989, **B46**, pp. 69–73
5 TOWNSEND, P. D.: 'An overview of ion-implanted optical waveguide profiles', *Nucl. Inst. Methods*, 1990, **B-46**, pp. 18–25
6 CHANDLER, P. J., FIELD, S. J., HANNA, D. C., SHEPHERD, D. P., TOWNSEND, P. D., TROPPER, A. C., and ZHANG, L.: 'Ion implanted Nd : YAG planar waveguide laser', *Electron. Lett.*, 1989, **25**, p. 985
7 TOWNSEND, P. D.: 'Optical waveguides formed by ion implantation in Al_2O_3 and $CaCO_3$'. Editions. de Phys. MRS, 1984, 'Induced defects in insulators', 1985, pp. 207–214
8 BURNETT, P. J., and PAGE, T. F.: 'Criteria for mechanical property modifications of ceramic surfaces by ion implantation', *Radiation Effects*, 1986, **97**, pp. 283–296
9 KELLY, R.: 'Phase changes in insulators produced by particle bombardment', *Nucl. Inst. Methods*, 1981, **182/183**, pp. 351–378
10 WHITE, C. W., MCHARGUE, C. J., SKLAD, P. S., BOATNER, L. A., and FARLOW, G. C.: 'Ion implantation and annealing of crystalline oxides', *Maters Science Reports*, 1988, **4**, pp. 41–146
11 MCHARGUE, C. J., SKLAD, P. S., and WHITE, C. W.: 'The structure of ion implanted ceramics', *NIM*, 1990, **B46**, pp. 79–88
12 DALAL, M. L., RAHMANI, M., and TOWNSEND, P. D.: 'UV absorption of ion implanted sapphire', *NIM*, 1988, **B32**, pp. 61–65
13 RAHMANI, M., ABU-HASSAN, L. H., TOWNSEND, P. D., WILSON, I. H., and DESTEFANIS, G. L.: 'Silver colloid formation in Ag^+ implanted $LiNbO_3$', *NIM*, 1988, **B32**, pp. 56–60
14 RAHMANI, M., and TOWNSEND, P. D.: 'Ag^+ implantation in Al_2O_3, $LiNbO_3$ and quartz', *Vacuum*, 1989, **39**, pp. 1157–1162
15 MCHARGUE, C. J., FARLOW, G. C., WHITE, C. W., WILLIAMS, J. M., APPLETON, B. R., and NAROMOTO, H.: 'The amorphization of ceramics by ion beams', *Materials Science and Engineering*, 1985, **69**, pp. 123–127
16 CHANDLER, P. J., and LAMA, F. L.: 'A new approach to the determination of planar waveguide profiles by means of a non-stationary mode index calculation', *Optica Acta*, 1986, **33**, pp. 127–143

EXPERIMENTAL OBSERVATION OF FORWARD STIMULATED BRILLOUIN SCATTERING IN DUAL-MODE SINGLE-CORE FIBRE

Indexing terms: Optical fibres, Optics, Scattering

Observation of intermodal forward stimulated Brillouin scattering at 514·5 nm in dual-mode optical fibres is reported. The FSBS signal is shifted by 16·6 MHz and, unlike in normal background SBS, does not depend significantly on the laser linewidth. The Brillouin gain in backward and forward directions is compared.

There has been a recent growth of interest in dual-moded (DM) optical fibres for a variety of nonlinear switching and modulation schemes.[1–4] The reason for this interest is twofold. First, optical fibres offer long interaction lengths, and second, dual-moded guiding structures offer two non-degenerate co-propagating optical modes at the same optical frequency. Forward stimulated Brillouin scattering (FSBS) between the LP_{01} and LP_{11} modes of a DM fibre is reported (briefly described recently).[5] Conventional Brillouin scattering in single-mode optical fibre can only occur between the forward and backward propagating modes, since these are the only two non-degenerate guided modes that exist. The wavelength of the acoustic phonon is then $\lambda_L/2n$ where λ_L is the pump wavelength and n the effective refractive index of the guided mode. Extensional acoustic waves travel at a phase velocity of $v_0 = 5760$ m/s in silica, yielding a Brillouin frequency shift of 32·4 GHz in a typical fibre at 514·5 nm. Acoustic waves at this frequency have very high losses ($\alpha_0 \sim 10^6\,m^{-1}$).

The SBS process is essentially a mutual support system for three waves: the pump, the Brillouin and the sound wave. The sound wave scatters (by Bragg diffraction) power from the pump into the Brillouin mode. These two optical signals interfere to produce moving interference fringes that phase match (if the conditions are correct) to the sound wave. Electrostriction then creates gain for the acoustic phonon, increasing its lifetime and hence its propagation distance.

The FSBS mechanism is similar in outline. Intermodal beating between the LP_{01} and PL_{11} modes of the dual-mode fibre gives rise to an interference pattern with regions of constructuve interference that alternate to and fro across the core. The period of this beat pattern is $L_b = 2\pi/(k_{01} - k_{11})$ where k_{01} and k_{11} are the wavevectors of the two fibre modes. When one of the modes is frequency shifted, the beat pattern will travel along the fibre at a velocity $v_F = f_F L_b$ where f_F is the frequency shift. If the velocity and beat period of this pattern correspond to those of a flexural fibre mode (i.e., if $L_b = \Lambda_F$, the acoustic wavelength) then electrostriction will feed optical energy into the flexural mode. The flexural wave itself causes micro-bending coupling between the two fibre modes, thereby increasing the visibility of the interference fringes and breaking the loop of cause and effect. A significant FSBS signal will appear in the second fibre mode if the pump power level in the launched mode is sufficient. The direction of the acoustic wave depends on whether the pump is launched in the fundamental or the LP_{11} mode. Since k_{11} is shorter in length than k_{01} and energy conservation requires that the stimulated Brillouin signal be downshifted in frequency, it may be shown that pumping in the LP_{01} (LP_{11}) mode results in a forward (backward) propagating flexural wave.[5,7]

The experimental details were as follows: An Ar^+ laser running single-mode at 514·5 nm was used to deliver light to 500 m of DM fibre (Fig. 1). To verify truly single-frequency operation, part of the laser output was split off and monitored directly at a photodiode and a confocal Fabry–Perot. A shutter system allowed independent monitoring of the light emerging from the fibre. After careful adjustment of the launching conditions, the frequency spectrum in Fig. 2 was obtained at the photodiode. A clear frequency component is apparent at 16·6 MHz; no such signal was present in the laser output. For our fibre parameters, $L_b = 0{\cdot}17$ mm at 514·5 nm; at $f_F = 16{\cdot}6$ MHz, a fibre cladding radius $a = 62{\cdot}5\,\mu$m and a shear velocity $v_t = 3764$ m/s, the parameter $af_F/v_t = 0{\cdot}28$, which places the interaction in the transition region between low and high frequency flexural waves.[6] The full theory[6] then yields $v_F \approx 0{\cdot}5v_0 = 2880$ m/s. The product of L_b and f_F gives an independent estimate of $v_F = 2822$ m/s; the excellent agreement confirms that FSBS is taking place.

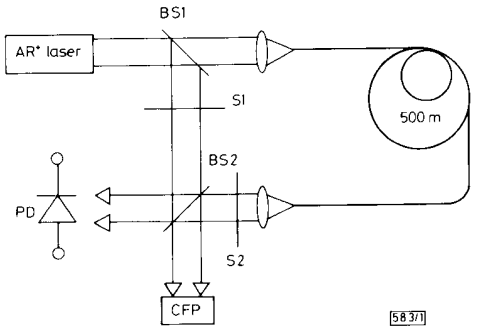

Fig. 1 *Experimental setup*

The threshold power for BSBS was slightly below that for FSBS (45 mW compared to 40 mW). The coherence length of the laser pump is known to play a crucial role in the BSBS threshold. In our experiment the Ar^+ laser was operated single frequency with an etalon to eliminate unwanted frequency components in the laser output. Its bandwidth was $\Delta\nu \sim 25$ MHz, corresponding to a coherence length of $(c/n\,\Delta\nu) \sim 8$ m. In FSBS, the two copropagating modes remain closely correlated over very long distances, with the consequence that coherence does not play a significant role. One major experimental consequence of this (not confirmed owing to limitations in the pump laser) is that FSBS would be easily

observable with multimode single-line laser light. The measured optical loss at 514·5 nm was $\alpha = 0{\cdot}005$, i.e., 20 dB/km. This means effective interaction lengths in the backward and forward cases of $L_{io} = \{1 - \exp(-\alpha c/2n\ \Delta\nu)\}/\alpha = 4$ m and $L_{iF} = \{1 - \exp(-500\alpha)\}/\alpha = 195$ m, respectively.

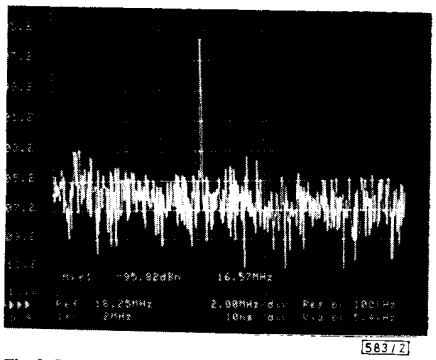

Fig. 2 *Spectrum*

It may be shown (to be presented in a separate detailed theoretical article)[7] that the ratio of the gain in FSBS to that in BSBS is

$$g_{BF}/g_{Bo} \approx \frac{\alpha_0 \Lambda_0}{2\alpha_F \Lambda_F}\left[\frac{r_{eq}}{a}\right]^4 \quad (1)$$

where r_{eq} is the effective mode radius of the light guided in the fibre and α_0 and α_F are the acoustic absorptions (per m) in the BSBS and FSBS cases. Notice the strong dependence on r_{eq}/a. The reasons for this are that the acoustic power is distributed over the entire fibre cross-section while the optical power is concentration in the core and that the induced electrostrictive moment scales with r_{eq} at constant optical power level. Under our experimental conditions $r_{eq} = 2{\cdot}3\,\mu$m. Taking $\alpha_0 = 10^{-6}\,\text{m}^{-1}$ and $\alpha_F \sim 0{\cdot}1\,\text{m}^{-1}$, the quantity g_{BF}/g_{Bo} has the value 2×10^{-2}. The ratio of the overall Brillouin gains in the two cases is then

$$(g_{BF} L_{iF}/g_{Bo} L_{io}) \sim 1$$

This agrees qualitatively with the experimental observation that the two thresholds occur at roughly the same pump power (and assumes that the spontaneous Brillouin and flexural wave seed signals are comparable in each case).

Acknowledgment: The authors are grateful to Prof. D. A. Jackson for the use of laboratory facilities.

P. ST. J. RUSSELL
D. CULVERHOUSE
F. FARAHI

Physics Laboratory
The University, Canterbury
Kent CT2 7NR, United Kingdom

18th June 1990

References

1 TRILLO, S., WABNITZ, S., and STEGEMAN, G. I.: 'Nonlinear codirectional guided wave mode conversion in grating structures', *J. Lightwave Technol.*, 1988, **LT-6**, pp. 971–976

2 RUSSELL, P. ST. J., and PAYNE, D. N.: 'Nonlinear switching in strongly coupled periodic dual waveguide couplers'. Topical Meeting on Nonlinear Guided-Wave Phenomena: Physics and Applications, Houston, Texas, 1989, Paper FC2-1

3 KIM, B. Y., BLAKE, J. N., ENGAN, H. E., and SHAW, H. J.: 'All-fiber acousto-optic frequency shifter', *Opt. Lett.*, 1986, **11**, pp. 389–391

4 FRIBERG, S. R., SILBERBERG, Y., OLIVER, M. K., ANDREJCO, M. J., SAIFI, M. A., and SMITH, P. W.: 'Ultra-fast all-optical switching in dual-core fiber nonlinear coupler', *Appl. Phys. Lett.*, 1987, **51**, pp. 1135–1137

5 CULVERHOUSE, D., RUSSELL, P. ST. J., and FARAHI, F.: 'Forward stimulated Brillouin scattering at 514·5 nm in dual-mode single core fibre'. Topical Meeting on Integrated Photonics Research, Hilton Head, South Carolina, 1990, Paper MC6

6 ENGAN, H. E., KIM, B. Y., BLAKE, J. N., and SHAW, H. J.: 'Propagation and optical interaction of guided acoustic waves in two-mode optical fibres', *J. Lightwave Technol.*, 1988, **LT-6**, pp. 428–436

7 RUSSELL, P. ST. J., CULVERHOUSE, D., and FARAHI, F.: 'Theory of forward stimulated Brillouin scattering in dual-mode single-core fibres', submitted to *IEEE J. Quantum Electron.*

OPTIMISED DESIGN FOR A 0·5 μm GATE LENGTH *n*-CHANNEL SOI MOSFET

Indexing term: Semiconductor devices and materials

Two dimensional device simulation has been used to optimise the design of an *n*-channel silicon-on-insulator MOSFET with an ultra thin film. The trade-off between SOI film thickness and film doping on the threshold voltage, inverse subthreshold slope and breakdown voltage is considered. The effect of carrier lifetime on the breakdown voltage is described. Use of a lightly doped drain gives a simulated breakdown voltage greater than 3·5 V for a transistor with a film thickness of 1000 Å and a gate length of 0·5 μm.

Introduction: Silicon-on-insulator (SOI) materials provide high density, high performance integrated circuits because of the total electric isolation of the silicon areas. They provide many attractive features for VLSI such as freedom from latch-up, low parasitic capacitance, reduced short channel effects, reduced alpha particle effects, applicability to 3D circuits and high drive currents giving high speed operation. With the current trends to reduce device dimensions into the submicron regime, SOI technology is an obvious contender. Designing a transistor with sub-micron gate length involves overcoming problems in trading off the threshold voltage, inverse subthreshold slope and breakdown voltage, whilst avoiding the onset of the SOI kink effect in the output characteristics.

It has been shown[1,2] that using ultra thin fully depleted films will both improve the inverse subthreshold slope and reduce the kink effect. Use of a thin film reduces the potential barrier at the boundary between the source and the SOI film, and allows holes generated by impact ionisation at the drain to cross into the source more easily. There is a tendency for thin film SOI transistors to have low breakdown voltages at or just below threshold since the potential barrier at the junction of the source and film has been reduced. This is caused by the action of the lateral *npn* bipolar transistor, where the base current is supplied by impact ionisation along the boundary of the drain.[3] The holes raise the potential in the channel (base) which increases the electron current by reducing the electron barrier at the source (emitter), until eventually the source junction becomes forward biased. The electron injection efficiency of the source is increased, raising the electron current, producing more impact ionisation at the drain (collector) and so on. Two possible methods of reducing the bipolar induced breakdown are to reduce impact ionisation at the drain, or to reduce the electron injection efficiency at the source junction. The former may be accomplished by reducing the peak electric field at the drain junction. This may be achieved using a lower doping gradient. The latter requires a decrease in the lifetime of the carriers in the film. Bipolar theory[4] indicates that a lower lifetime will increase recombination in the depleted film, and hence reduces the emitter efficiency.

In this letter the design criterion for optimising the inverse subthreshold slope and breakdown voltage of an *n*-channel thin film SOI MOSFET with a gate length of 0·5 μm is investigated. To allow potential implementation of SOI transistors in CMOS circuits, a nominal threshold voltage of 0·6 V was chosen. The design was evolved by a two dimensional solution of the semiconductor equations using the MINIMOS 4 program.[5] This program has been adapted so that it can be used to simulate SOI transistors fabricated in oxygen implanted SIMOX material, where it is appropriate to incorporate a substrate contact below the buried oxide. The program includes the effect of impact ionisation as a Chynoweth law, using coefficients which have been optimised for SOI transistors.[6]